Marcadores de conectividad cerebral dinámica en la Enfermedad de Alzheimer presintomática

Dynamical brain connectivity markers in presymptomatic Alzheimer's disease

Jazmín X. Suárez-Revelo[*1], John F. Ochoa-Gómez*[**1], Jon E. Duque-Grajales*[***1], y Carlos A. Tobón-Quintero*[****2]*

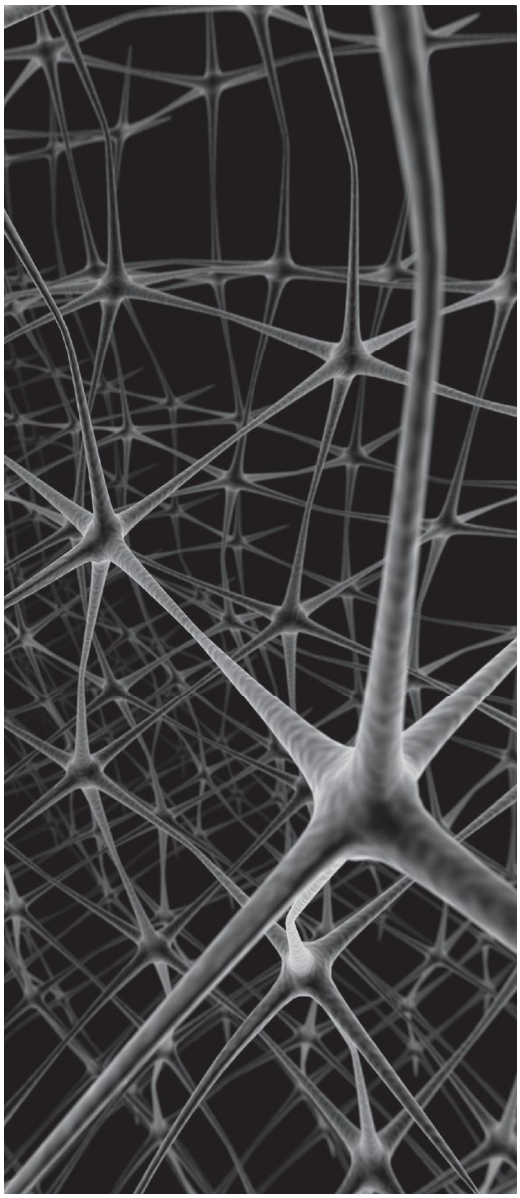

Resumen

La enfermedad de Alzheimer es la causa más frecuente de demencia, generalmente con inicio después de los 65 años. Sin embargo, hay algunas mutaciones genéticas que inducen la aparición de los síntomas neurocognitivos antes de esa edad. El estudio de los portadores de la mutación proporciona una oportunidad única para identificar los cambios preclínicos tempranos relacionados con la enfermedad. Los Potenciales Relacionados a Eventos son una herramienta poderosa utilizada para el estudio de sustratos neurales de la función cognitiva y el deterioro. El análisis de conectividad surge como una alternativa al enfoque típico de promedio de Potenciales Relacionados a Eventos. En el presente trabajo, dos grupos, portadores de la mutación y no portadores realizan una tarea de memoria durante el registro de Electroencefalografía. Se construyen grafos de la dinámica cerebral utilizando la Función de Transferencia Dirigida directa, calculada sobre señales promedio de ocho regiones de interés. Nuestros resultados muestran cómo el estudio dinámico de la conectividad podría ayudar a detectar cambios neuronales en la fase preclínica de la enfermedad de Alzheimer.

Palabras clave: Enfermedad de Alzheimer familiar, Electroencefalografía, Conectividad efectiva, Grafos cerebrales dinámicos.

* Grupo de investigación en Bioinstrumentación e Ingeniería Clínica (GIBIC), Departamento de Bioingeniería, Facultad de Ingeniería, Universidad de Antioquia, Medellín, Colombia jazmin.suarez@udea.edu.co,

** Grupo de investigación en Bioinstrumentación e Ingeniería Clínica (GIBIC), Departamento de Bioingeniería, Facultad de Ingeniería, Universidad de Antioquia, Medellín, Colombia john.ochoa@udea.edu.co,

*** Grupo de investigación en Bioinstrumentación e Ingeniería Clínica (GIBIC), Departamento de Bioingeniería, Facultad de Ingeniería, Universidad de Antioquia, Medellín, Colombia jon.duque@udea.edu.co,

**** Grupo de Neurociencias de Antioquia (GNA), Universidad de Antioquia, Medellín, Colombia. carlos.tobonq@udea.edu.co

Abstract

Alzheimer's disease is the most prevalent cause of dementia generally with an onset after the 65 years. However, there are some genetic mutations that induce the onset of the neurocognitive symptoms before that age. The study of mutation carriers provides a unique opportunity to identify early preclinical changes related to Alzheimer's disease. Event Related Potentials is a powerful tool used for the study of the neural substrates of cognitive function and deterioration. Connectivity analysis emerges as an alternative to the average approach typical in Event Related Potentials. In the current work, two groups of subjects (carriers and non-carriers of an AD mutation) performed a memory task during Electroencephalography recording. Dynamical brain graphs were built using the direct Directed Transfer Function calculated on the signals averaged of eight regions of interest. Our results show how the dynamical study of the connectivity could help to detect neuronal changes in preclinical stage of Alzheimer's disease.

keywords: Familial Alzheimer disease, Electroencephalography, Effective connectivity, Dynamical brain graphs.

I. Introduction

lzheimer's disease (AD) is the most prevalent cause of dementia, a neurodegenerative condition, generally with an onset after the 65 years [1]. Although is impossible to know which individuals will develop AD, some genetic mutations induce the occurrence of the disease [2], [3]. In Colombia exists a large family group with PSEN1 E280A mutation involved in the production of β-amyloid [4]. This mutation has an autosomal dominant inheritance with a mean age of 46.8 years at dementia onset [5]. The search of early biomarkers is an active research field because the efficacy of some AD therapies may depend of the initiation of treatment before clinical manifestation of the disease. In this way, the study of mutation carriers provides an unique opportunity to identify early changes related to predisposition to the disease [6], [7].

Electroencephalography (EEG) enables the research of early neurophysiological changes associated with the neurodegenerative processes. EEG has a high temporal resolution and represents a low cost, portable and non-invasive alternative to study the brain function [8]. The AD has been defined as a disconnection syndrome, and consequently network approaches based in graph theory could capture different features of the disease [9]–[13].

Recent studies in PSEN1 E280A mutation carriers give new evidences about connectivity changes that might be related to compensatory mechanisms [14]. In a visual recognition task were found differences only during the 200-300 ms highlighting the disease as a dynamical phenomenon [15].

In previous work, we found EEG quantitative changes in this population. During recordings of encoding in a memory task, theta frequency bands were lower in carriers compared with controls [16]. Here, we extend the study of this population with a graph theory based analysis. The aim of this work was to study the EEG signals as a dynamical process using graph theory in presymptomatic AD PSEN1 E280A mutation carriers and healthy non-carriers during a memory task.

Our main hypothesis is that connectivity in healthy non-carries subjects differ from PSEN1 E280A asymptomatic carriers and these differences can be used as a clinical marker of the disease in this population.

II. METHODS

A. Subjects

Subjects are members of the PSEN1 E280A mutation Colombian kindred: Participants with age between 18–34 years without cognitive impairment (Clinical Diagnostic Rating Scale (CDR) score of 0 and Folstein Mini-Mental State Examination (MMSE) score of 28 or higher). Fifteen Asymptomatic mutation carriers (ACr) and fifteen healthy non-carriers (Control) were matched for gender, age, and educational level (Table I). Informed consent for participation was obtained from all subjects according to the protocol approved by the Human Subjects Committee of the Universidad de Antioquia. All data were acquired by researchers who were blinded to the participant's genetic status. The exclusion criteria were severe physical illness, alcohol/drugs abuse, regular use of neuroleptics and antidepressants with anticholinergic action.

Table I. Demographic and neuropsychological characteristics of participants (ACr: asymptomatic mutation carriers; MMSE: mini-mental scale examination; SD: standard deviation; df: degrees of freedom).

	ACr	Control	T-Test
N	15	15	
Age (years)	27.8 (±4.0 SD)	31.5 (±5.8 SD)	T= -1.96 df= 14 P= 0.07
Gender (F/M)	9/6	9/6	
Education (years)	12.1 (±3.3 SD)	11.2 (±3.4 SD)	T= 0.82 df= 14 P= 0.43
MMSE	29.7 (±0.6 SD)	29.5 (±0.9 SD)	T= 0.68 df= 14 P= 0.51

B. EEG recordings

A Neuroscan unit amplifier (Neuroscan Medical System, Neurosoft Inc. Sterling, VA, USA) was used to record EEGs. EEG data were recorded (0.1-200 Hz bandpass) from 64 electrodes positioned according to the international 10-10 system with midline reference (recomputed to common average). A simultaneous electrooculogram (0.1±100 Hz bandpass) was also recorded.

Data were registered during an Event Related Potentials (ERP) experiment where participants performed a memory encoding task using color pictures of concrete and nameable objects. 50 stimuli were presented. Each trial began with a 1000 ms fixation character ("+") prior to the presentation of the stimuli. Then, stimuli were presented for 2000 ms followed by the question, "Do you like this item?" Subjects were then prompted to button press to signify their like/dislike judgment.

C. Signal pre-processing

Clean EEG was obtained from the implementation of automated preprocessing pipeline using MATLAB toolbox EEGLAB [17]. Data were filtered (1–50 Hz; FIR filter), bad channels were detected and interpolated using spherical splines. Then, data was segmented in epochs of 1.25 s and re-referenced to average. The EEG epochs with ocular, muscular, and other types of artifact were removed by a computerized automatic procedure based on linear trend, joint probability and kurtosis approach [18]. Independent component analysis enhanced by wavelet was used to correct eye blinks artifacts [19]. The last method

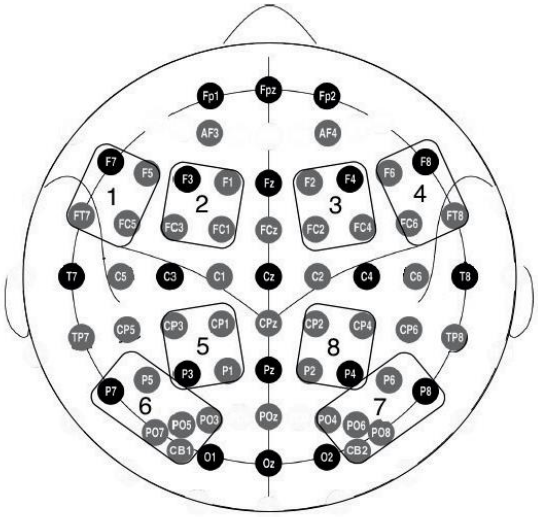

Figura 1. Electrode distribution according to 10-10 system and ROI selection.

applies a wavelet thresholding to the demixed independent components as an intermediate step, which enables recovering the neural activity present in artefactual components. In this case, we use a threshold of 0.1 that represents the probability that the component was neuronal. This probability was calculated by the Multiple Artifact Rejection Algorithm [20].

The corrected data was resampled to 200 Hz and used to calculate 8 regions of interest (ROI's) as the mean of the time series of the channels in each ROI (FigURA 1).

D. Direct Directed Transfer Function and Graph construction

In the current work the direct Directed Transfer Function (dDTF) was used as measure of connectivity. The dDTF may be considered as an extension of the Granger causality principle (effective connectivity) for an arbitrary number of channels [21]. The dDTF could be extended to study the connectivity in a dynamic way, even in cognitive tasks [22]. This kind of approach offers an insight into information processing in the brain, and may elucidate the origins of brain pathology.

For each subject a sliding-window Adaptive Multivariate Autoregressive (AMVAR) model was fitted to the data and the dDTF was estimated using the Source Information Flow Toolbox (SIFT) [21]. SIFT applies a wide range of methods for assessing effective connectivity between EEG signals. The length of the sliding-window was 250 ms. The parameters used to fit the model are shown in the Table II.

In each sliding-window the dDTF is calculated as follows:

$$d_{ij}^2(f) = n_{ij}^2(f) k_{ij}^2(f) \quad (1)$$

$$n_{ij}^2(f) = \frac{|H_{ij}(f)|^2}{\sum_f \sum_{m=1}^{k} |H_{im}(f)|^2} \quad (2)$$

$$k_{ij}(f) = \frac{\widehat{S_{ij}}(f)}{\sqrt{\widehat{S_{ii}}(f)\widehat{S_{jj}}(f)}} \quad (3)$$

$$\widehat{S_{ij}}(f) = S(f)^{-1} \quad (4)$$

Where f is the frequency, $n^2_{ij}(f)$ is the full frequency DTF (2), is the partial coherence (3), H_{ij} is the system transfer matrix obtained after the z-transform of the AMVAR model, and $S(f)$ is the spectral density matrix.

Table II AMVAR model parameters (mean ± standard deviation).

Parameter	Value
Model Order	9.27 ± 0.94
Window step	0.01 s
Window length	0.25 s
Consistency	(75.89 ± 0.57) %
Stability	100 %

The dDTF was analyzed in six frequency bands (delta: 1–4 Hz, theta: 4–8 Hz, alpha1: 8–10 Hz, alpha2: 10–13 Hz, beta: 13–30 Hz, and gamma: 30–50 Hz) for 126 intervals of 10 ms each one. The first interval started at the time of stimulus presentation. At each interval an 8x8 matrix was obtained where each entry (i,j) correspond to the connectivity between the ROI-i and the ROI-j. To simplify the statistical analysis, the measures were reduced to twelve intervals of 100 ms as the average of 10 intervals of 10 ms.

The new matrices were converted to ensemble graphs, that avoids the definition of a threshold for the comparison between groups [23]. Three graphs measures were obtained: node strength, node clustering coefficient, and network characteristic path length [24]. Node strength is the sum of weights of links connected to the node (5).

$$k_i^w = \sum_{j \in N} w_{ij} + \sum_{j \in N} w_{ji} \quad (5)$$

Where K^w_i is the node strength, N is the set of all nodes in the network and w_{ji} are the connection weights between node i and j.

The clustering coefficient is a measure of functional segregation which quantifies the fraction of intensities triangles around an individual node

and is equivalent to the fraction of the node's intensities neighbors that are also neighbors of each other [25] and is calculated as in (6):

$$k_i^w = \sum_{j \in N} w_{ij} + \sum_{j \in N} w_{ji} \qquad (6)$$

Where K^w_i and k^i_{in} are the out-degree and in-degree, respectively.

The characteristic path length is the average of shortest path length between all pairs of nodes in the network and is the most commonly used measure of functional integration [26]. It is calculated as in (7):

$$L^w = \frac{1}{N}\sum_{i \in N} \frac{\sum_{j \in N, j \neq i} d_{ij}^w}{N-1} \qquad (7)$$

Where k^i_{out} is the shortest weighted path length between *i* and *j*.

E. Statistical analysis

The main working hypothesis of this study was that the connectivity across time could differ in preclinical Alzheimer's disease compared with control subjects. To test this hypothesis an analysis of repeated measures using the two sample Hotelling's T-square test was conducted. This analysis was conducted for each frequency band and ROI separately. Additionally, a Two-sample Kolmogorov-Smirnov test was performed over the mean intervals of each measure to compare dynamical versus stationary functional connectivity. Statistical significance used for all tests was $\alpha = 0.05$. P values were corrected for multiple comparisons for each node using the Bonferroni correction method [27].

III. RESULTS

There were not differences in demographic information (age, gender and education) or neuropsychological examination (MMSE) (Table I) as expected given the asymptomatic condition of the population.

In static connectivity, differences were not found. For dynamical connectivity, significant differences are shown in Table III. We observed differences in alpha1 band for all measures: in node strength for ROI 2 and ROI 8, and clustering coefficient for ROI 8. Figura 2 and 3 illustrate the change of the graph measures for ROI 8 and ROI 2, respectively. ROI 8 has higher connectivity strength and a higher lustering coefficient after the 200 ms in ACr patients compared with Control subjects. Unlike to the ROI 8, in ROI 2 ACr has less connectivity strength than the Control group. In order to compare the graph analysis with the traditional ERP method, we evaluated the mean amplitude in time series for ROI 8 and ROI 2 and no statistical differences were found ($p > 0.05$). ACr shows a significant lower characteristic path length after 200 ms compared with Control group as shown in Figura 4.

Table III. *Hotelling`s T-square test results for ACr patients and Control subjects.* (ROI: region of interest; T2: Hotelling T-Squared test).

Measure	Band	ROI	T2	P-value
Node strength	Delta	2	41.6975	0.0001
		6	36.8252	0.0002
	Alpha1	2	108.0493	0.0009
		8	28.1575	0.0052
Node clustering coefficient	Alpha1	8	32.6850	0.0011
	Alpha2	8	29.0623	0.0039
Characteristic path length	Alpha1		30.2615	0.0026
	Alpha2		27.3268	0.0069
	Beta		21.5646	0.0427

IV. DISCUSSION

The previous results suggest a different behavior in connectivity measures for ACr relative to Control group during the encoding process, mainly in right parietal region (ROI 8) for alpha 1 band.

Studies with the mutation PSEN1 E280A have shown an alteration in brain function in presymptomatic disease cases. By estimating intracranial sources of evoked potentials (ERPs) in semantic processing, lower N400 amplitudes were found in carriers compared with presymptomatic carriers and noncarriers [28]. In another study, using high density ERPs to examine dynamic brain function in young presymptomatic carriers, found that despite an identical behavioral performance, the carriers showed lower positivity in frontal regions and increased positivity in occipital regions compared with control subjects. These measurements showed high sensitivity and specificity for predicting the presence of AD [15]. Our results show that the analysis of dynamic connectivity can also detect changes in the preclinical stage opening the possibility to new hypotheses in biomarkers research.

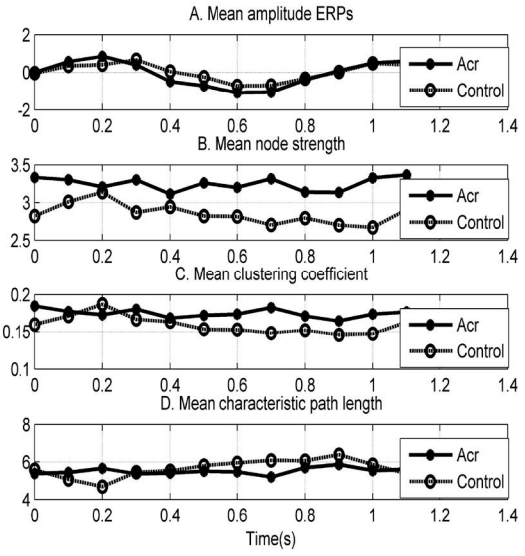

Figura 2. Mean ERPs (A), strength (B), and clustering coefficient (C) values in ROI 8 in alpha1 band for ACr and Control groups.

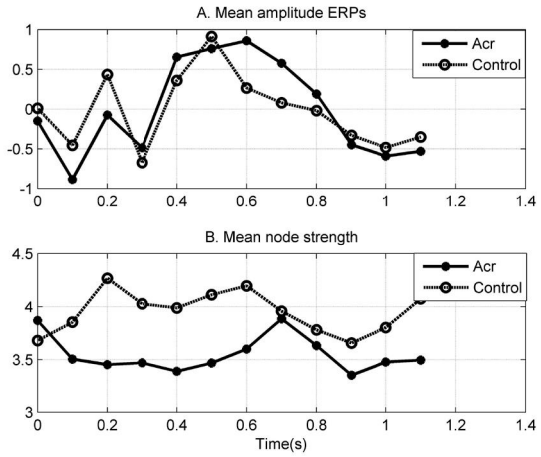

Figura 3. Mean ERPs (A) and strength (B) in alpha1 band for ACr and Control groups in ROI 2.

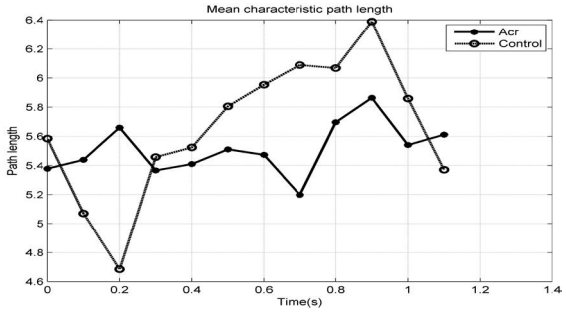

Figura 4. Mean characteristic path length in alpha1 band for ACr and Control groups.

Quantitative analysis of EEG (qEEG) also have showed changes in preclinical stages of the disease. The power characteristics on fast frequency bands (alpha and beta) enables an accurate discrimination between healthy and asymptomatic carriers groups and between patients with probable AD and asymptomatic carriers [16], [29].

Previous studies also shown an increase connectivity in mutation carriers in the theta and alpha1 bands [30], but only at global level. The proposed analysis allowed the detection of more specific differences by region also in the alpha band.

Graph analysis in AD has shown a loss of brain functional network topology, leading the network towards a more random topology, given by a reduction in clustering coefficient values and characteristic path length [31]–[33]. Our results

may suggest a network topology more complex in ACr group due higher clustering coefficient and lower characteristic path length values. This change in complexity, although could be a compensatory mechanism, might be related to a higher metabolic cost [34]. A study on cognitive effort during a working memory task found that greater effort cause emergence of a more globally efficient but less economical network configuration in fast frequency bands [35]. A similar phenomenon could be happening in ACr subjects.

In our work, we found that the analysis of dynamic connectivity measures in alpha band allows differentiation between these groups, but further studies are required to evaluate the discriminating power of these measures.

V. Conclusion

In this paper brain dynamics under a task of visual encoding in pre-symptomatic Alzheimer's disease was studied. The results show that the temporal analysis of functional connectivity, unlike the stationary analysis, is more sensible differentiating between carriers and non-carriers. Actually, it is only possible to establish that there are different behaviors of the measures for both groups. Future studies are needed to know in which time intervals the differences are higher.

Our results show how the dynamical study of the connectivity might help to detect neuronal changes in preclinical stage of Alzheimer's disease, something that open the possibility to use the measures as clinical markers in this population.

VI. Acknowledgment

This work was supported by Vicerrectoría de Investigación of Universidad de Antioquia (CODI), Project "Identificación de marcadores preclínicos de la mutación E280A de la enfermedad de Alzheimer a partir de medidas de conectividad en EEG", code PRG14-1-02.

Conflicts of interest

The authors do not declare conflict of interest.

References

[1] L. Minati, T. Edginton, M. G. Bruzzone, and G. Giaccone, "Current concepts in Alzheimer's disease: a multidisciplinary review.," *Am. J. Alzheimers. Dis. Other Demen.*, vol. 24, no. 2, pp. 95–121, 2009.

[2] L. Bertram and R. E. Tanzi, "Genetics of Alzheimer's Disease," *Neurodegeneration: The Molecular Pathology of Dementia and Movement Disorders: Second Edition.* pp. 51–61, 2011.

[3] E. Rogaeva, T. Kawarai, and P. S. George-Hyslop, "Genetic complexity of Alzheimer's disease: successes and challenges.," *J. Alzheimers. Dis.*, vol. 9, no. 3 Suppl, pp. 381–387, 2006.

[4] F. Lopera, A. Ardilla, A. Martínez, L. Madrigal, J. C. Arango-Viana, C. A. Lemere, J. C. Arango-Lasprilla, L. Hincapié, M. Arcos-Burgos, J. E. Ossa, I. M. Behrens, J. Norton, C. Lendon, A. M. Goate, A. Ruiz-Linares, M. Rosselli, and K. S. Kosik, "Clinical features of early-onset Alzheimer disease in a large kindred with an E280A presenilin-1 mutation," *J. Am. Med. Assoc.*, vol. 277, no. 10, pp. 793–799, 1997.

[5] A. Ardila, F. Lopera, M. Rosselli, S. Moreno, L. Madrigal, J. C. Arango-Lasprilla, M. Arcos, C. Murcia, J. C. Arango-Viana, J. Ossa, A. Goate, and K. S. Kosik, "Neuropsychological profile of a large kindred with familial Alzheimer's disease caused by the E280A single presenilin-1 mutation," *Arch. Clin. Neuropsychol. Off. J. Natl. Acad. Neuropsychol.*, vol. 15, no. 6, pp. 515–528, Aug. 2000.

[6] R. Sperling, E. Mormino, and K. Johnson, "The Evolution of Preclinical Alzheimer ' s Disease : Implications for Prevention Trials," *Neuron*, vol. 84, no. 3, pp. 608–622, 2014.

[7] J. B. Langbaum, A. S. Fleisher, K. Chen, N. Ayutyanont, F. Lopera, Y. T. Quiroz, R. J. Caselli, P. N. Tariot, and E. M. Reiman, "Ushering in the study and treatment of preclinical Alzheimer disease.," *Nat. Rev. Neurol.*, vol. 9, no. 7, pp. 371–81, Jul. 2013.

[8] C. Micanovic and S. Pal, "The diagnostic utility of EEG in early-onset dementia: a systematic review of the literature with narrative analysis," *J.*

neural Transm. (Vienna, Austria 1996), vol. 121, no. 1, pp. 59–69, Jan. 2014.

[9] Y. Ouchi and M. Kikuchi, "A review of the default mode network in aging and dementia based on molecular imaging," *Rev. Neurosci.*, vol. 23, no. 3, pp. 263–268, 2012.

[10] Y. He, Z. Chen, G. Gong, and A. Evans, "Neuronal networks in Alzheimer's disease," *Neurosci. a Rev. J. bringing Neurobiol. Neurol. psychiatry*, vol. 15, no. 4, pp. 333–350, Aug. 2009.

[11] E. T. Bullmore and D. S. Bassett, "Brain graphs: graphical models of the human brain connectome.," *Annu. Rev. Clin. Psychol.*, vol. 7, pp. 113–40, Jan. 2011.

[12] A. Hafkemeijer, J. van der Grond, and S. A. R. B. Rombouts, "Imaging the default mode network in aging and dementia," *Biochim. Biophys. Acta - Mol. Basis Dis.*, vol. 1822, no. 3, pp. 431–441, Mar. 2012.

[13] T. Xie and Y. He, "Mapping the Alzheimer's brain with connectomics," *Front. Neuropsychiatr. Imaging Stimul.*, vol. 2, p. 77, 2012.

[14] Y. T. Quiroz, A. E. Budson, K. Celone, A. Ruiz, R. Newmark, G. Castrillon, F. Lopera, and C. E. Stern, "Hippocampal hyperactivation in presymptomatic familial Alzheimer's disease.," *Ann. Neurol.*, vol. 68, no. 6, pp. 865–875, Dec. 2010.

[15] Y. T. Quiroz, B. a Ally, K. Celone, J. McKeever, a L. Ruiz-Rizzo, F. Lopera, C. E. Stern, and a E. Budson, "Event-related potential markers of brain changes in preclinical familial Alzheimer disease.," *Neurology*, vol. 77, no. 5, pp. 469–75, Aug. 2011.

[16] J. E. Duque-Grajales, C. Tobón, C. P. Aponte-Restrepo, J. F. Ochoa-Gomez, C. Muñoz-Zapata, A. M. Hernández-Valdivieso, Y. T. Quiroz-Zapata, and F. Lopera, "Quantitative EEG analysis disease during resting and memory task in carriers and non-carriers of PS-1 E280A mutation of familial Alzheimer´s," *Rev. CES Med.*, vol. 28, no. 2, pp. 165–176, 2014.

[17] A. Delorme and S. Makeig, "EEGLAB: An open source toolbox for analysis of single-trial EEG dynamics including independent component analysis," *J. Neurosci. Methods*, vol. 134, pp. 9–21, 2004.

[18] A. Delorme, T. J. Sejnowski, and S. Makeig, "Enhanced detection of artifacts in EEG data using higher-order statistics and independent component analysis," *Neuroimaging*, vol. 34, no. 4, pp. 1443–1449, 2007.

[19] N. P. Castellanos and V. a. Makarov, "Recovering EEG brain signals: Artifact suppression with wavelet enhanced independent component analysis," *J. Neurosci. Methods*, vol. 158, pp. 300–312, 2006.

[20] I. Winkler, S. Haufe, and M. Tangermann, "Automatic Classification of Artifactual ICA-Components for Artifact Removal in EEG Signals," *Behav. Brain Funct.*, vol. 7, no. 1, p. 30, 2011.

[21] A. Delorme, T. Mullen, C. Kothe, Z. Akalin Acar, N. Bigdely-Shamlo, A. Vankov, and S. Makeig, "EEGLAB, SIFT, NFT, BCILAB, and ERICA: New tools for advanced EEG processing," *Comput. Intell. Neurosci.*, vol. 2011, 2011.

[22] K. J. Blinowska, M. Kamiński, A. Brzezicka, and J. Kamiński, "Application of directed transfer function and network formalism for the assessment of functional connectivity in working memory task," *Philos. Trans. R. Soc. London A Math. Phys. Eng. Sci.*, vol. 371, no. 1997, Jul. 2013.

[23] S. E. Ahnert, D. Garlaschelli, T. M. A. Fink, and G. Caldarelli, "Ensemble approach to the analysis of weighted networks.," *Phys. Rev. E. Stat. Nonlin. Soft Matter Phys.*, vol. 76, no. 1 Pt 2, p. 16101, Jul. 2007.

[24] M. Rubinov and O. Sporns, "Complex network measures of brain connectivity: uses and interpretations.," *Neuroimage*, vol. 52, no. 3, pp. 1059–69, Sep. 2010.

[25] J. P. Onnela, J. Saramäki, J. Kertész, and K. Kaski, "Intensity and coherence of motifs in weighted complex networks," *Phys. Rev. E - Stat. Nonlinear, Soft Matter Phys.*, vol. 71, 2005.

[26] D. Watts and S. H. Strogatz, "Collective dynamics of 'small-world' networks.," *Nature*, vol. 393, no. 6684, pp. 440–2, 1998.

[27] C. E. Bonferroni, *Teoria statistica delle classi e calcolo delle probabilità.* Libreria internazionale Seeber, 1936.

[28] M. a Bobes, Y. F. García, F. Lopera, Y. T. Quiroz, L. Galán, M. Vega, N. Trujillo, M. Valdes-Sosa, and P. Valdes-Sosa, "ERP generator anomalies in presymptomatic carriers of the Alzheimer's disease E280A PS-1 mutation.," *Hum. Brain Mapp.*, vol. 31, no. 2, pp. 247–65, Feb. 2010.

[29] R. Rodriguez, F. Lopera, A. Alvarez, Y. Fernandez, L. Galan, Y. Quiroz, and M. A. Bobes, "Spectral Analysis of EEG in Familial Alzheimer's Disease with E280A Presenilin-1 Mutation Gene.," *Int. J. Alzheimers. Dis.*, vol. 2014, p. 180741, Jan. 2014.

[30] J. Ochoa, F. Sánchez, C. Tobón, J. Duque, Y. Quiroz, F. Lopera, and M. Hernandez, "Effective Connectivity Changes in Presymptomatic Alzheimer's Disease with E280A Presenilin-1 Mutation Gene," in *VI Latin American Congress on Biomedical Engineering CLAIB 2014, Paraná, Argentina 29, 30 & 31 October 2014 SE - 130*, vol. 49, A. Braidot and A. Hadad, Eds. Springer International Publishing, 2015, pp. 508–511.

[31] E. J. Sanz-Arigita, M. M. Schoonheim, J. S. Damoiseaux, S. a R. B. Rombouts, E. Maris, F. Barkhof, P. Scheltens, and C. J. Stam, "Loss of 'small-world' networks in Alzheimer's disease: graph analysis of FMRI resting-state functional connectivity.," *PLoS One*, vol. 5, no. 11, p. e13788, Jan. 2010.

[32] C. J. Stam, W. de Haan, A. Daffertshofer, B. F. Jones, I. Manshanden, A. M. van Cappellen van Walsum, T. Montez, J. P. A. Verbunt, J. C. de Munck, B. W. van Dijk, H. W. Berendse, and P. Scheltens, "Graph theoretical analysis of magnetoencephalographic functional connectivity in Alzheimer's disease.," *Brain*, vol. 132, no. Pt 1, pp. 213–24, Jan. 2009.

[33] K. Supekar, V. Menon, D. Rubin, M. Musen, and M. D. Greicius, "Network analysis of intrinsic functional brain connectivity in Alzheimer's disease.," *PLoS Comput. Biol.*, vol. 4, no. 6, p. e1000100, Jun. 2008.

[34] E. Bullmore and O. Sporns, "The economy of brain network organization.," *Nat. Rev. Neurosci.*, vol. 13, no. 5, pp. 336–49, May 2012.

[35] M. G. Kitzbichler, R. N. a Henson, M. L. Smith, P. J. Nathan, and E. T. Bullmore, "Cognitive effort drives workspace configuration of human brain functional networks.," *J. Neurosci.*, vol. 31, no. 22, pp. 8259–8270, 2011.